Biol. Chem., Vol. 386, pp. 41–52, January 2005 • Copyright © by Walter de Gruyter • Berlin • New York. DOI 10.1515/BC.2005.006

Characterization of the glyoxalases of the malarial parasite *Plasmodium falciparum* and comparison with their human counterparts

Monique Akoachere[1], Rimma Iozef[1], Stefan Rahlfs[1], Marcel Deponte[1], Bengt Mannervik[2], Donald J. Creighton[3], Heiner Schirmer[4] and Katja Becker[1,*]

[1] Interdisciplinary Research Center, Heinrich-Buff-Ring 26-32, Justus-Liebig University, D-35392 Giessen, Germany
[2] Department of Biochemistry, Uppsala University, Biomedical Center, Box 576, S-751 23 Uppsala, Sweden
[3] Department of Chemistry and Biochemistry, University of Maryland, Baltimore County, Baltimore, MD 21228, USA
[4] Biochemistry Center, Im Neuenheimer Feld 504, Ruprecht-Karls University, D-69120 Heidelberg, Germany

* Corresponding author
e-mail: becker.katja@gmx.de

Abstract

The glyoxalase system consisting of glyoxalase I (GloI) and glyoxalase II (GloII) constitutes a glutathione-dependent intracellular pathway converting toxic 2-oxoaldehydes, such as methylglyoxal, to the corresponding 2-hydroxyacids. Here we describe a complete glyoxalase system in the malarial parasite *Plasmodium falciparum*. The biochemical, kinetic and structural properties of cytosolic GloI (cGloI) and two GloIIs (cytosolic GloII named cGloII, and tGloII preceded by a targeting sequence) were directly compared with the respective isofunctional host enzymes. cGloI and cGloII exhibit lower K_m values and higher catalytic efficiencies (k_{cat}/K_m) than the human counterparts, pointing to the importance of the system in malarial parasites. A Tyr185Phe mutant of cGloII shows a 2.5-fold increase in K_m, proving the contribution of Tyr185 to substrate binding. Molecular models suggest very similar active sites/metal binding sites of parasite and host cell enzymes. However, a fourth protein, which has highest similarities to GloI, was found to be unique for malarial parasites; it is likely to act in the apicoplast, and has as yet undefined substrate specificity. Various S-(*N*-hydroxy-*N*-arylcarbamoyl)glutathiones tested as *P. falciparum* Glo inhibitors were active in the lower nanomolar range. The Glo system of *Plasmodium* will be further evaluated as a target for the development of antimalarial drugs.

Keywords: drug development; enzyme inhibition; glutathione derivatives; methylglyoxal; molecular modeling.

Introduction

The glyoxalase (Glo) system, a glutathione (GSH)-dependent detoxification system involved in the conversion of toxic 2-oxoaldehydes to the corresponding non-toxic 2-hydroxyacids, is composed of two enzymes: glyoxalase I (GloI; EC 4.4.1.5) and glyoxalase II (GloII; EC 3.1.2.6). GloI converts the non-enzymatically produced hemithioacetal from a 2-oxoaldehyde and GSH to a thiolester of GSH, which can then be readily hydrolyzed by GloII, producing a 2-hydroxyacid and regenerating GSH (Figure 1; Thornalley, 1993).

Physiological substrates (2-oxoaldehydes) of the glyoxalase system are: glyoxal formed in lipid peroxidation and glycation reactions; methylglyoxal arising from triose phosphates and thus glycolysis, ketone body metabolism and threonine catabolism; and 4,5-dioxovalerate generated from 5-aminolevulinate and α-ketoglutarate. Previous studies have proven the electrophilic binding of 2-oxoaldehydes to guanyl residues of DNA and RNA, as well as to lysyl, arginyl and cysteinyl residues of proteins (Lo et al., 1994; Vaca et al., 1994). This leads to mutagenesis, apoptosis, protein cross-linking and degradation, as well as to the synthesis and production of pro-inflammatory cytokines (Thornalley, 1996, 1998). 2-Oxoaldehydes mediate the formation of advanced glycation end products (AGEs) which can lead to pathophysiological complications in diabetes and are known to be cytostatic at low concentrations and cytotoxic at high concentrations (Thornalley, 1996, 1998).

The glyoxalase system has been characterized in various organisms, including man and other mammals (Marmstål et al., 1979; Biswas et al., 2002; Mearini et al., 2002), fish (Antognelli et al., 2003), higher plants (Crowder et al., 1997), yeast (Frickel et al., 2001), bacteria (Clugston and Honek, 2000), trypanosomes (Irsch and Krauth-Siegel, 2004) and nematodes (Sommer et al., 2001). The cytosol is the main cellular location of the Glo system; however, some isoenzymes have been reported to contain signal targeting sequences for mitochondria and even plastids (Cordell et al., 2004). The ubiquitous distribution of the glyoxalase system, the presence of several isoenzymes in a single organism, and the high sequence similarity of Glo from different sources indicate the importance of the detoxification of 2-oxoaldehydes –

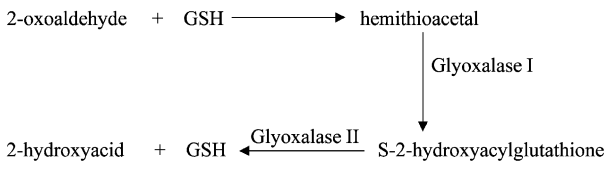

Figure 1 The glyoxalase system.

Table 1 Cloning and overexpression of human and *P. falciparum* glyoxalase genes.

Gene, accession no.		Primer sequence	Restriction site	PCR	Expression vector	*E. coli* strain	Overexpression
cGloI, AF486284		Iozef et al., 2003	Iozef et al., 2003	Iozef et al., 2003	pQE30	M15	Overnight at 30°C after induction with 0.25 mM IPTG at OD_{600}=0.3 OD_{600} using LB medium containing 8 mM $MgSO_4$, 1 mM $ZnSO_4$ and 10 mM Tris, pH 7.5
	Sense	Iozef et al., 2003					
	Antisense	Iozef et al., 2003					
GILP, NP 703709				94°C, 30 s 65°C, 45 s 72°C, 60 s 25 cycles	pQE30	M15 BL21	Overnight at 24–30°C after induction with 0.25 mM IPTG at OD_{600} 0.7–0.8 using LB medium containing 8 mM $MgSO_4$, 10 mM Tris, pH 7.5
	Sense	CGCGGGATCCAAACTTTTT GTAGTCGTTATATTTGTTC	*Bam*HI				
	Antisense	GCGCAAGCTTTTATTTGTCTT TTAAGTAAACATTATATCCG	*Hin*dIII				
tGloII, AF486285				94°C, 30 s 50°C, 45 s 72°C, 90 s 35 cycles	pQE30	M15	6 h at 37°C after induction with 1 mM IPTG at OD_{600}=0.7 using LB medium containing 8 mM $MgSO_4$, 10 mM Tris, pH 7.5
	Sense	CGCGGGATCCGCACAA GAAATATCAAATTTAG	*Bam*HI				
	Antisense	GCGCAAGCTTTTATGAG GCTTTAAAATTATCC	*Hin*dIII				
cGloII, AY494055				94°C, 30 s 60°C, 30 s 72°C, 90 s 35 cycles	pQE30	XL-I	4 h at 37°C after induction with 1 mM IPTG at OD_{600}=0.5 using LB medium
	Sense	CGCGGGATCCAAGCCATGCG CACAAGTACTTGTAGTGC	*Bam*HI				
	Antisense	CGCGGAGCTCTTAAAAATTAT TTTTTAATTGTCTTAATTTAT	*Sac*I				
Human *GloI*, NP_006699				94°C, 30 s 64°C, 30 s 72°C, 45 s 35 cycles	pQE30	BL21 (DE3)	Overnight at 30°C after induction with 0.25 mM IPTG at OD_{600}=0.3 using ZY medium containing 1 mM $ZnSO_4$
	Sense	CGCGGGATCCAAGCCATGCG CACAAGTACTTGTAGTGC	*Bam*HI				
	Antisense	CGCGAAGCTTCTACATT AAGGTTGCCATTTTG	*Hin*dIII				
Human *GloII*, CAA62483			Ridderström et al., 1996	Ridderström et al., 1996	pKKD	JM109	Overnight at 37°C after induction with 0.25 mM IPTG at OD_{600}=0.3 using ZY medium
	Sense	Ridderström et al., 1996					
	Antisense	Ridderström et al., 1996					

Restriction endonuclease sites added to the primer sequences are underlined.

```
PfGloIC        -----------------NYKNITN-------FSQTMIRVKNPEKSLYFYIHILGMKLIHV  208
HsGloI         MAEPQPPSGGLTDEAALSYCSDADPSTKDFLLQQTMLRVKDPKKSLDFYTRVLGMTLIQK   60
PfGloIN        -----------MAQEISNLVKKYNVT-----WQQTMLRIYDPKETVEFYEKNFGMINIHT   44
                                  .  .  :        .***:*: :*:::: ** : :**  *:

PfGloIC        KHCSD--FSLYFLKSNYACAENNKEMIEDQSNKNTNEIYDFNSLKNSYQTDEDYENFKQS  266
HsGloI         CDFPIMKFSLYFLAY-----EDKNDIPK---EKDEKLAWALSRK----------------   96
PfGloIN        YHFNEYNFSLYFLITPPYDEEERKKLPEPNTKESEKYLWNLNTV----------------   88
                     ****** .     *:.... .  . .    .: :.

PfGloIC        WEPVLELTHNHGTEDDDNFSYHNGNTE-PRGFGHIGFLVNDLENYCKELETLNVTFKKKVT 326
HsGloI         --ATLELTHNWGTEDDETQSYHNGNSD-PRGFGHIGIAVPDVYSACKRFEELGVKFVKKPD 154
PfGloIN        ---CLELTYNHNSQEK----LSNGNNENDRGFGHIAFNCNDVIEQCDNLFKKNVKFHKLPH 142
                   ****:*. ::::..  . :***.:  ******::   *: . *..:   .*.* *

PfGloIC        EGLMKNIAFIYDPDNYVIELIQRDTSFIAK 356
HsGloI         DGKMKGLAFIQDPDGYWIEILNPNKMATLM 184
PfGloIN        ETKMKTIGFALDPNNYWIEIVKRSNQVKWK 172
                  ** ::*: **: *:***.
```

Figure 2 Alignment of N- and C-terminal halves of *P. falciparum* glyoxalase I with human glyoxalase I.
Residues involved in the formation of the active Zn^{2+} coordination site are indicated by white letters, while those involved in the formation of the hydrophobic binding pocket are shadowed. Putative metal-defining inserts (Sukdeo et al., 2004) are underlined.

produced from physiological reactions – in biological systems (Thornalley, 1993).

Blood stages of the malarial parasite *Plasmodium falciparum* are mainly responsible for the clinical manifestations of the disease. After sequencing the *P. falciparum* genome, it is still unclear whether the citric acid cycle and oxidative phosphorylation are significantly involved in energy production of the blood stages (Gardner et al., 2002). In any case, the parasite exhibits high glycolytic activity to cover energy demands resulting from its high proliferation rate (Jacobasch et al., 1990). This activity is indicated by an approximately 75-fold increase in glucose consumption in *P. falciparum*-infected erythrocytes in comparison with normal erythrocytes (Sherman, 1979) and exposes the parasite to higher fluxes of methylglyoxal produced by the spontaneous decomposition of triose phosphates (glyceraldehyde-3-phosphate and dihydroacetone phosphate) during the triose phosphate isomerase reaction of glycolysis (Thornalley, 1996). The anti-malarial activity of Glo inhibitors was demonstrated by the growth inhibition caused by S-*p*-bromobenzylglutathione diethyl ester with IC_{50} values in the lower micromolar range (Thornalley et al., 1994). Selective inhibition of the Glo system leading to 2-oxoaldehyde stress within the parasite therefore provides a promising chemotherapeutic approach to the treatment of malaria. New chemotherapeutic approaches are urgently needed to fight against the increasing drug resistance of the parasite, and to reduce the 2 million malaria deaths per year and the increased geographical spread of the disease (Olliaro, 2001; Greenwood and Mutabwinga, 2002).

Recently, we characterized a glyoxalase I from *P. falciparum* (Iozef et al., 2003). This cGloI belongs to a group of large glyoxalases I earlier characterized in yeast (Frickel et al., 2001), and later found in plants (Clugston et al., 1998), *Plasmodium yoelii* and in insects such as *Anopheles gambiae* and *Drosophila melanogaster* (Iozef et al., 2003). Genes of these large glyoxalases are almost twice the size of the smaller glyoxalases, of which human GloI is a good example. The amino acid sequences of the N- and C-terminal halves of their monomeric gene products are homologous to each other and to the two subunits of homodimeric small glyoxalases I (Ridderström and Mannervik, 1996a). These observations led to the gene duplication hypothesis on the evolution of these large glyoxalases, which was further supported by the fact that the recombinantly produced C-terminal half of cGloI showed glyoxalase I activity (Iozef et al., 2003).

We now have identified the genes of a second putative GloI (*GILP*) as well as of two GloII forms (*tGloII* and *cGloII*) in *P. falciparum*. Here, we report the comparative structural and functional analysis of the four putative glyoxalases with their isofunctional human counterparts. First inhibitor studies serve as a basis for further elucidating the functions of the glyoxalase system in *P. falciparum* and for estimating its potential as target for the development of antimalarial drugs.

Results

Recombinant production of *P. falciparum* glyoxalases

Screening the *Plasmodium falciparum* genome sequencing database with different known *GloI* and *GloII* genes resulted in the identification of a second putative GloI gene from chromosome 6 and two putative *GloII* genes from chromosome 4 and chromosome 12, respectively. Designed perfect match primers were employed in polymerase chain reactions (PCR) (Table 1) using *P. falciparum* cDNA as the template and the resulting products of expected size were cloned into the expression vector pQE30 and sequenced. The sequences were in full agreement with the respective sequences found in the genomic database.

The basic characterization of the cGloI gene product (see Figure 2 for sequence information referring to the 3-D model) has been reported previously (Iozef et al., 2003). The *GILP* gene from chromosome 6 consists of 924 bp and its gene product of 307 amino acids contains an N-terminal apicoplast targeting sequence with high probability (>98%, PATS 1.2.1N; Zuegge et al., 2001). High sequence identities were obtained with the respective proteins from other *Plasmodium* species (e.g., 67% identity with *P. yoelii*) but only low identities were found with proteins from other species, the highest value being 25% identity with *Arabidopsis thaliana*. The gene product

```
HsGloII         ------------------------------------------------------------
AtcGloII        ------------------------------------------------------------
PfcGloII        ------------------------------------------------------------
ScGloII         ------------------------------------------------------------
AtmGloII        MPVISKASSTTTNSSIPSCSRIGGQLCVWPGLRQLCLRKSLLYGVMWLLSMPLKTLRGAR  60
PftGloII        ------------------------------------------------------------

HsGloII         -----------------MKVEVLPALTDNYMYLVIDDETKEAAIVDPVQPQKVVDAARKH  43
AtcGloII        -----------------MKIFHVPCLQDNYSYLIIDESTGDAAVVDPVDPEKVIASAEKH  43
PfcGloII        -------------MKPCAQVLVVPVLNDNFSYVIIDEKTKKAASIDPVEPDKVLKRIETA  47
ScGloII         -------------MQVKSIKMRWESGGVNYCYLLSDSKNKKSWLIDPAEPPEVLPELTED  47
AtmGloII        KTLKITHFCSISNMPSSLKIELVPCSKDNYAYLLHDEDTGTVGVVDPSEAAPVIEALSRK 120
PftGloII        ---------------MCTNTIIIPFYKDNYSYIFYDDK-EEGIVVDPADYN-IINDISKK  43
                                              *: *:. *...     :** :   ::

HsGloII         G-VKLTTVLTTHHHWDHAGGNE------KLVKLESGLKVYGGD---DRIGALTHKITHLS  93
AtcGloII        Q-AKIKFVLTTHHHWDHAGGNE------KIKQLVPDIKVYGGSL--DKVKGCTDAVDNGD  94
PfcGloII        N-VELEYVLCTHHHYDHSGGN------IRMRELKQNIKVVGSAY--EPTPGVNEKVYDGQ  98
ScGloII         EKISVEAIVNTHHHYDHADGNADILKYLKEKNPTSKVEVIGGSK--D-CPKVTIIPENLK 104
AtmGloII        N-WNLTYILNTHHHDDHIGGN-------AELKERYGAKVIGSAVDKDRIPGIDILLKDSD 172
PftGloII        ENIKIKHVLCTHKHSDHNNGNQ--------YYYEKNINVYGIKEY--DNKYINQDISNLT  93
                   .:  :: **:* ** .**                :* *     .          .

HsGloII         TLQVG-SLNVKCLATPCHTSGHICYFVSKPGGSEP------PAVFTGDTLFVAGCGKFYE 146
AtcGloII        KLTLGQDINILALHTPCHTKGHISYYVNGKEG-EN------PAVFTGDTLFVAGCGKFFE 147
PfcGloII        IIRLG-ELNIKAIHAPCHTKGHILYYVYKTDEAKQEDHKYKPILFTGDTLFIAGCGRFFE 157
ScGloII         KLHLG-DLEITCIRTPCHTRDSICYYVKDPTTDER-------CIFTGDTLFTAGCGRFFE 156
AtmGloII        KWMFA-GHEVRILDTPGHTQGHISFYFPGSAT-----------IFTGDLIYSLSCGTLSE 220
PftGloII        HFQIN-NFKINIFLSNFHSKNQVSYLIENDNNKSK-----KNIFFTGDFLFISGIGKNFE 147
                   .    ::  : :  *: . : : .      .         .**** ::  . *   *

HsGloII         GTADEMCKALLEV-----LGRLPPDTRVYCGHEYTINNLKFARHVEPGNAAIREKLAWAK 201
AtcGloII        GTAEQMYQSLCVT-----LAALPKPTQVYCGHEYTVKNLEFALTVEPNNGKIQQKLAWAR 202
PfcGloII        GSAKDMFKNIEK------VKNMRKETLIYCGHEYTLNNLRFALSIENDNEYMKNKLNEVT 211
ScGloII         GTGEEMDIALNNSILETVGRQNWSKTRVYPGHEYTSDNVKFVRKIYP--QVGENKALDEL 214
AtmGloII        GTPEQMLSSLQK------IVSLPDDTNIYCGRENTAGNLKFALSVEPKNETLQSYATRVA 274
PftGloII        QDNEDLYNSINKL-----KLLDKQNIYIFCGHEYTLDNLKFALTVDSTNKNLLSFYDHVV 202
                   .::   :                 :: *:* *  *:.*.  :   .    .

HsGloII         EKYSIGEPTVPS--TLAEEFTYNPFMRVREKTVQQHAGETDPVTTMRAVRRE-----KDQ 254
AtcGloII        QQRQADLPTIPS--TLEEELETNPFMRVDKPEIQEKLGCKSPIDTMREVRNK-----KDQ 255
PfcGloII        EKLKNKEHSVPS--TIEEENLINPFFRT--HCYVNKFNMNDEIKILDKLRQ--------- 258
ScGloII         EQFCSKHEVTAGRFTLKDEVEFNPFMRLEDPKVQKAAGDTNNSWDRAQIMDK-----LRA 269
AtmGloII        HLRSQGLPSIPT--TVKVEKACNPFLRISSKDIRKSLSIPDSATEAEALRRI-----QRA 327
PftGloII        NS-NKNYPTVPT--LLEHEYLYNPFLRCDQNDVRKSIDLYAKKKNIKIQQESDYIVILRL 259
                .         .    :  *   ***:*  .    .

HsGloII         FKMPRD-- 260
AtcGloII        WRG----- 258
PfcGloII        LKNNF--- 263
ScGloII         MKNRM--- 274
AtmGloII        RDRF---- 331
PftGloII        MKDNFKAS 267
```

Figure 3 Alignment of glyoxalases II.
Residues involved in binding of the substrate S-lactoyl-glutathione as shown for the human enzyme (Cameron et al., 1999b; Ridderström et al., 2000) are shadowed; the active site motif THxHxDH is boxed; two other conserved histidines required for zinc binding at the active site are indicated by white letters. GenBank accession numbers are given in parentheses: HsGloII, human glyoxalase II (CAA62483); AtcGloII, cytoplasmic *Arabidopsis thaliana* glyoxalase II (NM_111922); PfcGloII, *Plasmodium falciparum* cytoplasmic glyoxalase II (AY494055, this paper); ScGloII, S*accharomyces cerevisiae* (CAA71335); AtmGloII, mitochondrial *Arabidopsis thaliana* (NP_565999); PftGloII, *Plasmodium falciparum* targeted glyoxalase II (AF486285, this paper); the sequence of an N-terminally truncated form (55 aa) is given in this alignment. This short form of the protein was approximately 3.5-fold more active than the full-length protein.

(without His-tag, with targeting sequence) had a calculated molecular mass of 35.8 kDa, an isoelectric point at pH 8.59 and an $\varepsilon_{280\ nm}$ value of 33.6 mM^{-1} cm^{-1}.

The *tGloII* and *cGloII* genes from chromosomes 12 and 4 consist of 840 and 792 bp, respectively. Alignments of the amino acid sequences of *P. falciparum* glyoxalases II with those from other species showed identities of up to 32% (tGloII with *Gallus gallus* and *Cicer arietinum*) and 43% (cGloII with man and *Danio rerio*) (Figure 3). tGloII contains an N-terminal putative targeting sequence that was deleted in the cloning process to improve the solubility and stability of the protein. As deduced from its DNA sequence, tGloII is composed of 322 amino acids; the N-terminally truncated active form of the protein has 267 amino acids with a molecular mass of 31.8 kDa and an isoelectric point at pH 7.25. cGloII is composed of 263 amino acids with a molecular weight of 30.5 kDa and an isoelectric point at pH 7.64. The extinction coefficients ε at 280 nm were 27.12 and 17 mM^{-1} cm^{-1} for tGloII and cGloII, respectively.

Freshly transformed *E. coli* cells were employed for overexpression of the *P. falciparum* Glo genes (Table 1) and, as shown in Table 2, the hexahistidyl-tagged recombinant proteins were purified on Ni-NTA columns. cGloI

Table 2 Purification of *P. falciparum* and human glyoxalases.

Enzyme	First purification		Second purification		Yield (mg/l)
	Column	Elution	Column	Elution	
cGloI	S-C6-GSH in 10 mM Tris-HCl, pH 7.8	5 mM S-C6-GSH	Ni-NTA	100–200 mM imidazole	3
GILP	Ni-NTA	50–75 mM imidazole	–	–	5
tGloII	S-C6-GSH in 10 mM Tris, pH 7.8	3 M NaCl	Ni-NTA	50 mM imidazole	0.2
cGloII	Ni-NTA	30–200 mM imidazole	–	–	5
Human GloI	S-C6-GSH in 10 mM Tris-HCl, pH 7.8	5 mM S-C6-GSH	Ni-NTA	30–50 mM imidazole	0.5
Human GloII	S-C6-GSH in 10 mM MOPS, pH 7.2	3 M NaCl	–	–	2

S-C6-GSH, S-hexylglutathione; –, second purification not necessary. Washing steps on Ni-NTA columns were carried out with 50 mM sodium phosphate buffer, pH 8.0, containing 300 mM NaCl. Imidazole concentrations used during elution were diluted in the same buffer. Washing and elution steps for all GloI forms on S-hexylglutathione columns contained 200 mM NaCl.

Table 3 Kinetic properties of *P. falciparum* and human glyoxalase I enzymes.

Glyoxalase I	K_m (μM)	k_{cat} (min^{-1})	Specific activity (U/mg)	k_{cat}/K_m ($M^{-1}s^{-1}$)
cGloI	28±3	6637	150	4.0×10^6
Human GloI	90±10	2375	110	0.44×10^6

All values were obtained at 30°C. The *P. falciparum* glyoxalase I-like protein (GILP) was not active under the conditions tested (see the Results section).

Table 4 Kinetic properties of *P. falciparum* and human glyoxalase II enzymes.

Glyoxalase II	K_m (μM)	k_{cat} (min^{-1})	Specific activity (U/mg)	k_{cat}/K_m ($M^{-1}s^{-1}$)
tGloII	225±25	3860	117	0.29×10^6
cGloII	100±10	7175	226	1.19×10^6
Human GloII	248±25	2782	96	0.19×10^6

All values were obtained at 25°C. K_m values obtained at 37°C were 190 μM for cGloII, 208 μM for human GloII and 463 μM for the cGloII Tyr185Phe mutant.

and tGloII were pre-purified on an S-hexylglutathione agarose column. Yields and experimental details are shown in Table 2.

After overexpression in *E. coli* M15 cells, the gene product of the glyoxalase I-like protein (GILP) was insoluble. We therefore proceeded to clone and overexpress in *E. coli* BL21 cells three shorter variants of the *GILP* gene in order to remove the N-terminal apicoplast signal sequence from the gene products. Gene products of these shorter variants designated Δ20GILP, Δ23GILP and Δ43GILP lacked the first 20, 23 and 43 amino acids of the complete GILP sequence, respectively. These variants were soluble and could be purified to homogeneity on Ni-NTA columns with yields of approximately 5 mg per liter of cell culture.

Kinetic characterization

The kinetic characterization of cGloI has previously been reported by Iozef et al. (2003). As shown in the present study, addition of $ZnSO_4$ during the overexpression of cGloI resulted in increased catalytic activity and a decreased K_m value. In addition, the former measurements were carried out under conditions of excess methylglyoxal (MGO) and the assumption that glutathione (GSH) would be readily converted to the MGO-GSH hemithioacetal (Vander Jagt et al., 1972; Iozef et al., 2003). In the present study, the substrate concentrations in each assay were calculated on the basis of the dissociation constant of the MGO-GSH adduct (Ridderström and Mannervik, 1996b). Differences in protein quality and the assay system chosen thus explain the kinetic values obtained here. In direct comparison with human GloI, cGloI showed higher k_{cat} and lower K_m values (Table 3).

Different N-terminally truncated variants of GILP were successfully overexpressed in *E. coli* and purified. Unfortunately, none of these variants showed GloI activity under the various conditions tested. Buffers tested were: (i) 100 mM potassium phosphate, 0–300 mM KCl, pH 7.0, 6.6 or 6.0; (ii) 100 mM HEPES, 1 mM EDTA, pH 7.4; (iii) 50 mM Tris, pH 7.4; and (iv) 100 mM MOPS, 1 mM EDTA, pH 6.0 or 6.7. The addition of several metals ($ZnCl_2$, $NiCl_2$, $MnCl_2$, $CoCl_2$, $FeCl_2$, $FeCl_3$) in concentrations up to 100 μM or the addition of 0.5 mg/ml BSA to stabilize GILP did not lead to detectable activity either. The GloI substrates tested were the methylglyoxal-GSH and glyoxal-GSH hemithioacetal adducts.

Both *P. falciparum* glyoxalases II were capable of hydrolyzing S-D-lactoylglutathione to D-lactate and GSH with a pH optimum of pH 7.6–7.8 for tGloII and 7.2–7.8 for cGloII. Their kinetic properties, along with those of human GloII obtained in our laboratory, are shown in Table 4.

Inhibition studies

The inhibitory effects of S-(*N*-hydroxy-*N*-arylcarbamoyl)glutathione derivatives on both *P. falciparum* and human glyoxalases are shown in Table 5. These derivatives, being structural analogs of S-D-lactoylglutathione,

Table 5 IC_{50} and K_i values of S-(*N*-aryl-*N*-hydroxycarbamoyl)glutathiones on human and *P. falciparum* glyoxalases.

Glutathione derivative	cGloI		Human GloI		tGloII		cGloII		Human GloII	
	IC_{50} (μM)	K_i (μM)	IC_{50} (μM)	K_i (μM)	IC_{50} (μM)	K_i (μM)	IC_{50} (μM)	K_i (μM)	IC_{50} (μM)	K_i (μM)
HPC-GSH	10	ND	2.5	ND	185	ND	6	6	10	8
HCPC-GSH	0.11	0.08	0.09	0.05	30	50	2	0.7	1	0.7
HBPC-GSH	0.06	0.06	0.06	0.03	20	30	1.6	0.5	0.85	0.7–1

Values represent the mean of three independent determinations. ND, not determined; HPC-GSH, S-(*N*-hydroxy-*N*-phenylcarbamoyl)glutathiones; HCPC-GSH, S-(*N*-hydroxy-*N*-chlorophenylcarbamoyl)glutathiones; and HBPC-GSH, S-(*N*-hydroxy-*N*-bromophenylcarbamoyl)glutathiones.

showed K_i values for cGloI in the nanomolar range [see Figure 4A for S-(*N*-hydroxy-*N*-bromophenylcarbamoyl)-glutathione, HBPC-GSH] and for tGloII and cGloII in the micromolar range. When carrying out assays with these compounds as substrates in the absence of S-D-lactoyl-glutathione, no activity of cGloII could be observed at concentrations of up to 1 mM.

S-*p*-Bromobenzylglutathione competitively inhibited cGloI with a K_i value of 20 μM (Figure 4B). Human GloI was inhibited to a much greater degree, with a K_i value of 0.17 μM.

When tGloII was tested in inhibition assays with S-propylglutathione, S-hexylglutathione and S-(*p*-azidophenacyl)glutathione, K_i values of 1.9, 1.5 and 1.3 mM, respectively, were obtained. cGloII was even less sensitive to the compounds (data not shown). S-(*p*-Azidophenacyl)glutathione slightly activated the enzyme at concentrations of 0.2–1 mM.

Metal ion analysis

A metal content of up to 1.2 zinc and 0.1 nickel ions was obtained for cGloI (Iozef et al., 2003). According to sequence alignments, particular putative inserts responsible for defining GloI metal specificity to Zn^{2+} were found to be present in cGloI (Figure 2; Sukdeo et al., 2004). However, metal-coordinating residues were not entirely conserved in GILP and accordingly the metal content measured was negligible. Furthermore, the gene fusion demonstrated for *cGloI* (Iozef et al., 2003) does not apply to *GILP*.

The Zn^{2+}/metal binding motif T-H-X-H-X-D-H, as well as two additional histidine residues required for zinc binding, are conserved in both *P. falciparum* GloIIs (Figure 2). tGloII showed a Zn^{2+} ion content of 1.7±0.3, with insignificant amounts of other metals tested. cGloII had a rather low metal content of 0.05 and 0.26 for Zn^{2+} and Fe^{2+}, respectively. This indicated that the enzyme was not completely saturated with metals at its active site. We therefore tested GloII activity using buffers enriched with Zn^{2+}, Fe^{2+}, Fe^{3+}, Ni^{2+}, Ca^{2+} and Cu^{2+} ions, respectively. Only Zn^{2+} activated the enzyme by a factor of approximately 2.

Cell culture experiments

It is worth noting that potent inhibitors of glyoxalases are usually GSH derivatives that, as a result of the acidic nature of GSH, are not membrane-permeable; therefore, prodrug derivatives are used. The dialkylester prodrug of the inhibitor depends on the presence of unspecific intracellular esterases to generate the active drugs within the cell (Lo and Thornalley, 1992; Kavarana et al., 1999); the alkylsulfoxide depends on an acyl interchange with GSH within the cell (Hamilton et al., 1999). IC_{50} values of 30 and 10 μM were obtained for S-(*N*-hydroxy-*N*-chlorophenylcarbamoyl)glutathione HCPC-GSH diethyl ester and S-(*N*-hydroxy-*N*-arylcarbamoyl) HCPC-sulfoxide, respectively. Hemolysis could be observed when higher concentrations of both prodrugs were employed.

In extracts from isolated trophozoites of the *P. falciparum* strain Dd2, the specific activity of glyoxalase I and glyoxalase II was 0.2 and 1.0 U/mg, respectively. Treatment with 10 μM S-*p*-bromobenzylglutathione cyclopentyl diester, a potent GloI inhibitor, in a parallel culture (see materials and methods) led to 0.2 U/mg GloI and 0.7

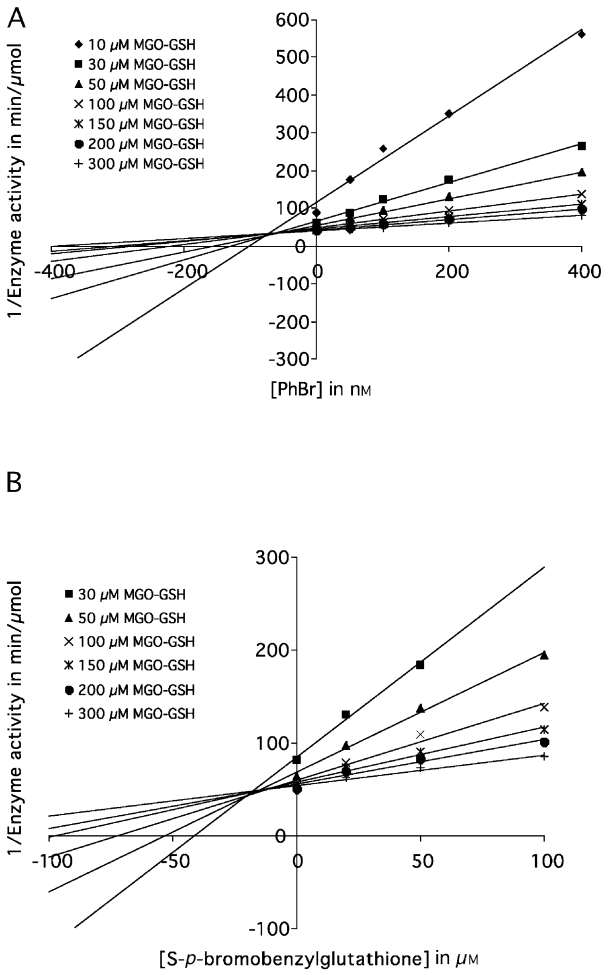

Figure 4 Dixon plots comparing competitive inhibition of (A) HBPC-GSH and (B) S-*p*-bromobenzylglutathione on *P. falciparum* glyoxalase I using the methylglyoxal-GSH adduct as substrate.

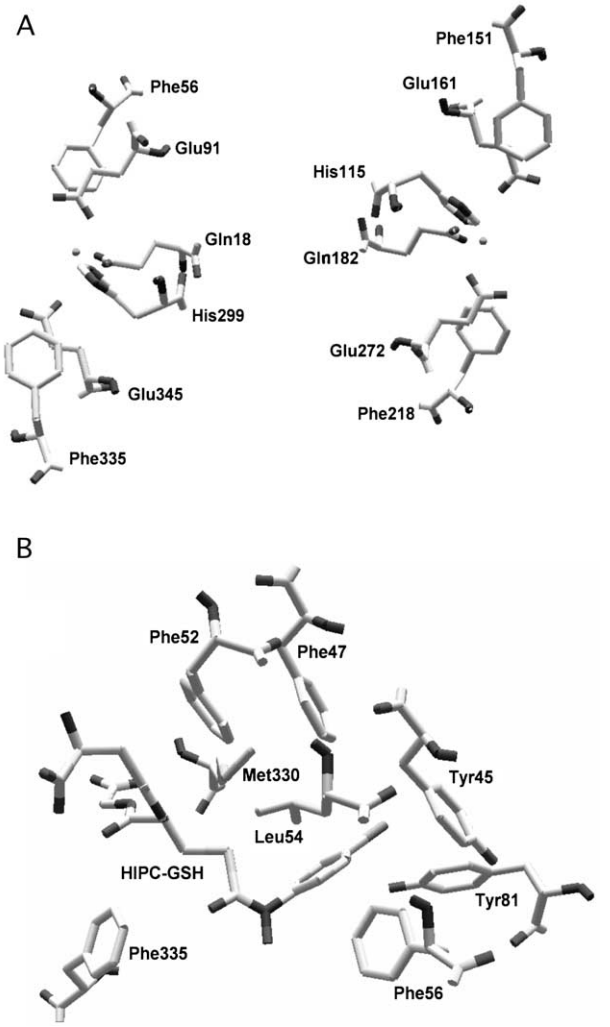

Figure 5 Model of the active sites and hydrophobic binding pocket of GloI based on the crystal structure of human GloI (Cameron et al., 1999a).
(A) The putative active sites of monomeric GloI with each containing a zinc ion (given as sphere). (B) Model of the putative hydrophobic binding pocket of monomeric cGloI.

U/mg GloII, respectively. The lack of induction of the glyoxalase system by the S-*p*-bromobenzylglutathione cyclopentyl diester might be explained by the fact that the *P. falciparum* enzymes, in contrast to human GloI, are not significantly affected by the inhibitor.

Plasmodium falciparum glyoxalase structure prediction

Models of cGloI, tGloII and cGloII were generated based on the crystal structures of the human glyoxalases I and II, respectively. Monomeric cGloI comprises two potential active sites, which are presumably very similar to the active sites of the human homodimer (Figures 2 and 5A). Gln18, Glu91, His299, and Glu345 coordinate the first zinc ion, and His115, Glu161, Gln182, and Glu272 bind a zinc ion at the second active site. As in yeast GloI, both active sites presumably act independently of each other (Frickel et al., 2001). Most of the residues involved in the formation of a hydrophobic binding pocket at the active site of human GloI (Kalsi et al., 2000) are also conserved in cGloI (Figures 2 and 5B). Conserved residues of the hydrophobic binding pocket in cGloI are Phe47, Phe52, Leu54, Phe56, Leu85, Phe335 and Met330. Cys60, Ile88 and Leu160′ (of the other subunit) in human GloI are replaced by Tyr45, Tyr81 and Ile333 in cGloI, respectively. Moreover, we observed greater binding affinity (reflected by lower K_i values) to cGloI with increasing hydrophobicity of the S-(*N*-hydroxy-*N*-arylcarbamoyl)glutathiones. This supports the hypothesis postulated by Kalsi et al. (2000) that occupancy of this pocket maximizes polar interactions between the enzyme and the bound enediol analogues. Despite the sequence similarities, a complete model of cGloI could not be generated due to a distance of 2.5 nm between Met138 and Ser25′ of human GloI, which are aligned to Lys172 and Tyr174 of cGloI. In addition, the residues corresponding to Met1–Pro24 of human GloI are missing in cGloI. Thus, the real structure of monomeric cGloI is likely to differ significantly from the human dimeric enzyme. Such significant differences could be exploited in the synthesis of specific inhibitors of cGloI. It was not possible to generate a model of GILP based on human GloI due to limited sequence similarity.

Structures and calculated force-field energy values (-8.8 MJ/mol) for tGloII and cGloII are very similar to the template used (Figure 6). The residues coordinating two

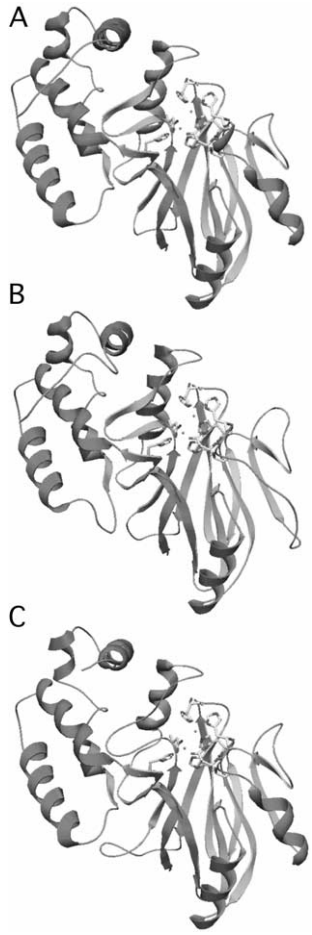

Figure 6 Model of tGloII and cGloII based on the crystal structure of human GloII (Cameron et al., 1999b).
Residues coordinating two zinc ions are highlighted. (A) Structure of human GloII showing an N-terminal domain, containing predominantly β-strands similar to metallo-β-lactamases, and a smaller second domain comprising predominantly α-helices; (B) model of tGloII; and (C) model of cGloII.

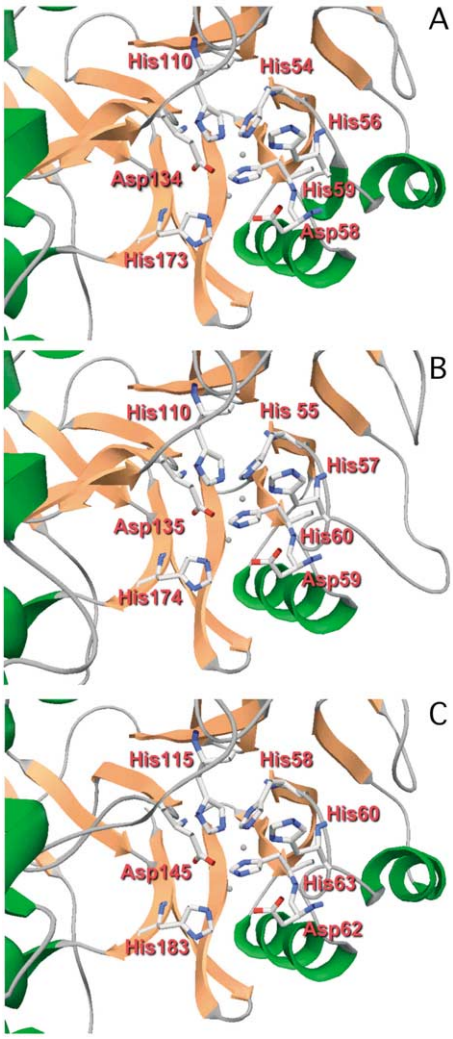

Figure 7 Model of the metal binding site of tGloII and cGloII based on the crystal structure of human GloII (Cameron et al., 1999b).
Residues coordinating two zinc ions are highlighted. (A) Structure of human GloII; (B) model of tGloII; and (C) model of cGloII.

zinc ions at the active site are conserved and the resulting metal binding site is also very similar for the three glyoxalases II (Figures 3 and 7). However, several residues contributing to the glutathione-binding site differ between tGloII, cGloII and human GloII (Figure 8). Arg249, Lys143 and Lys252 are thought to interact with the carboxylate group of the glycine of glutathione. In tGloII, two of these basic residues are replaced by Gln249 and Asp252. Tyr145 of human GloII is replaced by Phe, as is also the case for many other glyoxalases II (Cameron et al., 1999b), whereas Tyr175 and Lys143 are conserved or replaced by Arg, respectively.

Discussion

In recent years the glyoxalase system has attracted increasing attention as a chemotherapeutic target for antitumour drug development. Several compounds interfering with the glyoxalase system have been shown to inhibit the growth of cancer cells *in vitro* and *in vivo* (Hamilton and Creighton, 1992; Creighton et al., 2003). Blood stages of the malarial parasite *Plasmodium falciparum* are highly proliferative and of high glycolytic activity, and thus depend on the glyoxalase system for the detoxification of methylglyoxal. Inhibition of this system within the parasite therefore provides a promising chemotherapeutic strategy (Thornalley et al., 1996).

GloI is a member of the vicinal oxygen chelate metalloenzyme family (Armstrong, 2000), and contains a paired βαβββ motif providing a metal coordination environment. The reaction types catalyzed include isomerization (glyoxalase I containing Zn^{2+} and/or Ni^{2+}), epimerization (methylmalonyl-CoA epimerase with Co^{2+}), oxidative cleavage of C-C bonds (extradiol dioxygenase, $Fe^{2+}$and/or Mn^{2+}), and nucleophilic substitutions (fosfomycin resistance proteins, Mn^{2+}, Mg^{2+}).

As revealed by sequence similarities and the X-ray crystal structure of human GloII, GloII is a member of the relatively newly defined metallohydrolase family containing the β-lactamase fold consisting of a four-layered β sandwich (Cameron et al., 1999b; Daiyasu et al., 2001). This superfamily also includes class B β-lactamase, arylsulfatase, an mRNA 3′-processing protein, a DNA cross-link repair enzyme, an alkylphosphonate uptake-related protein, CMP-*N*-acetylneuraminate hydroxylase, and insecticide hydrolases.

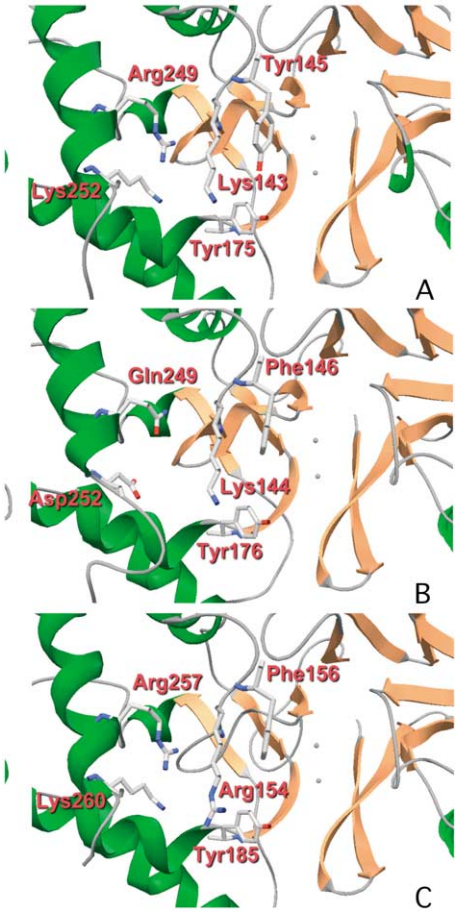

Figure 8 Model of the glutathione-binding site of tGloII and cGloII based on the crystal structure of human GloII (Cameron et al., 1999b).
Residues involved in glutathione-binding are highlighted. (A) Structure of human GloII; (B) model of tGloII; and (C) model of cGloII.

As reported here, a complete glyoxalase system in *P. falciparum* comprising at least one GloI and two GloII isoenzymes has been characterized in our laboratory, and direct structural and functional comparisons with the isofunctional human host enzymes have been carried out.

cGloI and cGloII seem to be localized in the cytosol and act together as the major defense line against toxic 2-oxoaldehydes. In direct comparison with the respective host enzyme, cGloI shows a three-fold lower K_m value for methylglyoxal-GSH and slightly higher specific activity. In addition, the K_m value for cGloII is at least two-fold lower than that for human GloII and the k_{cat} value is more than two-fold higher. This indicates the need for efficient methylglyoxal detoxification in the malarial parasites. Both glyoxalases start to act in the lower micromolar range. The involvement of Tyr185 in the catalysis of cGloII was studied by site-directed mutagenesis. In analogy to human GloII (Ridderström et al., 2000) Tyr185 was proven to contribute to substrate binding, as reflected by a 2.5-fold increase in K_m.

tGloII carries a putative apicoplast import sequence and GILP is also preceded by a targeting sequence that might direct the protein to the apicoplast and/or the mitochondrion. This fact points to the possibility that the apicoplast, a prokaryote-derived cell organelle of *Plasmodium*, possesses glyoxalase activity and pathways generating toxic 2-oxoaldehydes. The catalytic properties of tGloII are comparable to human GloII. For GILP, however, no typical glyoxalase activity could be determined, with the physiological substrate remaining unknown. This fact is of particular interest, since GILP is only present and highly conserved in *Plasmodium* species. Highest sequence identities with proteins from other species were only 25% with *A. thaliana*, other plants having a monomeric large GloI, and photosynthetic bacteria, which have the dimeric form of small GloI. Furthermore, they point to the 'green' origin of *Plasmodium*. The function of GILP will be studied in further detail.

As previously shown, cGloI is a zinc-dependent enzyme (Iozef et al., 2003), which was further supported by the fact that overexpression in the presence of Zn^{2+} enhanced catalytic activity. GILP, however, did not bind significant amounts of metal ions and has no known central metal coordinating motifs either. tGloII was shown to be clearly Zn^{2+}-dependent, whereas cGloII had a rather low metal content of 0.05 and 0.26 atoms for Zn^{2+} and Fe^{2+}, respectively, and could be slightly activated by zinc. A zinc dependency has been reported for other GloII enzymes, e.g., for GloII from *Arabidopsis thaliana* (Crowder et al., 1997). In addition, other metals were shown to bind to GloII, namely iron and manganese, especially if the enzymes were produced in media enriched with these metals (Wenzel et al., 2004). The Zn/metal binding motif T-H-X-H-X-D-H, as well as the two other histidines required for zinc binding, are conserved in both *P. falciparum* GloIIs (Figures 2 and 6).

As a basis for further inhibitor development, we tested different S-(*N*-hydroxy-*N*-arylcarbamoyl)glutathione derivatives as *P. falciparum* GloI and GloII inhibitors. The compounds acted as strong competitive inhibitors of both Glo isoenzymes – on cGloI in the nanomolar range and on tGloII and cGloII in the micromolar range (Table 5). The inhibitors had originally been synthesized as inhibitors of GloI and slow substrates of GloII based on the very low GloII activity in tumor cells compared to normal cells (Murthy et al., 1994). The fact that the S-(*N*-hydroxy-*N*-arylcarbamoyl)glutathiones are substrates for mammalian glyoxalase II but not for *P. falciparum* glyoxalases II indicates that these compounds might selectively inhibit human glyoxalases, since normal human cells – in contrast to malarial parasites – would be able to hydrolyze the inhibitor. Tight binding of the inhibitors to the enzymes arises in part from mimicking the stereoelectronic features of the enediol intermediate formed from the methylglyoxal-glutathione-hemithioacetal that acts as a substrate for GloI, and also in part by the interaction of the *N*-aryl substituent with a hydrophobic pocket at the active site of GloI (Cameron et al., 1999a). The latter reason is clearly supported by the increase in binding affinity with increasing hydrophobicity of the inhibitors, which is further supported by our data. An alignment of the amino acid sequences of human GloI and cGloI showed that 80% of the residues involved in the composition of the hydrophobic binding pocket of human GloI are conserved in cGloI (Figures 1 and 4B). HBPC-GSH showed a lower K_i value for cGloII than for human GloII and could thus serve as a starting point for the development of more selective inhibitors.

Unexpectedly, S-*p*-bromobenzylglutathione, the diethyl ester prodrug form that has been demonstrated to inhibit the growth of *P. falciparum in vitro* (Thornalley et al., 1994), is a weak cGloI inhibitor with a K_i value of 20 μM. Much stronger competitive inhibition is observed for human GloI, with a K_i value in the region of 0.17 μM (Aronsson et al., 1981; Murthy et al., 1994; and results from this study). This strongly indicates that the antiparasitic effects of the compound are not primarily based on the inhibition of the parasite glyoxalase system, but of other enzymes, or on interference with the human methylglyoxal detoxification in red cells.

With the characterization of a complete, functional, and most likely essential glyoxalase system in *Plasmodium falciparum*, a novel potential target for antimalarial drug development has become accessible. First inhibitor studies revealing inhibition in the nanomolar range and the identification of a novel GloI-like enzyme, which is likely to be unique for malarial parasites, represent the most promising steps towards the possibility of specific interference with this pathway. Furthermore, the emergence of suitable prodrug forms of the S-(*N*-hydroxy-*N*-arylcarbamoyl)glutathiones, which mask the acidic nature and thus allow membrane permeation, are most encouraging for successful drug development.

Materials and methods

Materials

All chemicals used were of the highest available purity and were obtained from Roth (Karlsruhe, Germany), Merck (Frankfurt am Main, Germany) or Sigma/Aldrich (Steinheim, Germany). The expression system QIA-express [vector pQE30, *E. coli* host strain M15, and nickel-nitrilotriacetic acid (Ni-NTA) matrices for purification of His-tagged protein] was purchased from Qiagen

(Hilden, Germany). PCR primers were obtained from MWG-Biotech (Ebersberg, Germany), and the sequencing reactions were carried out on an ABI Prism 310 Genetic Analyzer.

Cloning, overexpression and protein purification

Complete open reading frames of a second putative *GloI* gene on chromosome 6 and two putative *GloII* genes on chromosomes 4 and 12 were identified by on-line screening of the *P. falciparum* genome project (www.ncbi.nlm.nih.gov/Malaria/plasmodium-blcus.html). N- and C-terminal primers were designed from the sequence of the 5′- and 3′-ends of the genes, respectively. A *P. falciparum* gametocyte cDNA library from the strain 3D7 was used as template for the PCR amplification. All three genes were cloned into the expression vector pQE30 and – as for *cGloI* (Iozef et al., 2003) – overexpressed in *E. coli*. Primers used for the amplification of the human *GloI* gene were designed from the gene sequence obtained from the GenBank™/EMBL Data Bank (accession no. NP_006699). A human lung cDNA library was kindly provided by Dr. Lutz Schomburg (Charité, Berlin, Germany) and used as a template. The human *GloI* gene was then cloned into pQE30 and overexpressed using *E. coli* BL21(DE3) plus S cells. The gene encoding cytosolic human GloII in the vector pKK-D (Ridderström et al., 1996) was overexpressed in *E. coli* JM109. After recombinant production, all six proteins were purified to homogeneity using S-hexylglutathione and Ni-NTA affinity matrices. Tables 1 and 2 delineate gene cloning, overexpression and purification of the gene products used in this study.

The Tyr185Phe mutant of cGloII was generated by site-directed mutagenesis using standard PCR with *Pfu* DNA polymerase using the following primers: OPfG4Ys 5′-GCG GAC ATG AGT TTA CCC TTA ATA ATT TAA GG-3′ and OPfG4Yas 5′-CCT TAA ATT ATT AAG GGT AAA CTC ATG TCC GC-3′. The expression clone of *cGloII* was used as a template. The resulting PCR product was sequenced to make sure that no unwanted mutations had been introduced.

Enzymatic assays

Kinetic measurements were carried out using a thermostatted Hitachi U-2001 UV-Vis spectrophotometer. GloI activity was determined by the rate of formation of the thiol ester S-D-lactoylglutathione [from the methylglyoxal (MGO)-glutathione (GSH) hemithioacetal] at 240 nm, with an extinction coefficient of ε=3.37 mM^{-1} cm^{-1} (Ridderström and Mannervik, 1996b). The GloI standard assay mixture was defined as follows: 100 mM potassium phosphate (with 100 mM KCl for cGloI), pH 7.0 and 0.01–0.5 mM of the hemithioacetal (MGO-GSH) were incubated for 5 min and the reaction was started by adding GloI. The total assay volume was 1 ml. For a desired concentration of MGO-GSH, the required concentrations of MGO and glutathione (GSH) were calculated from the equations below; excess free GSH in the assay was 0.1 mM. K_d=([MGO]×[GSH])/[MGO-GSH]; the dissociation constant $K_{d(MGO\text{-}GSH)}$ was 3 mM (24), [MGO_{total}] in the assay was ([MGO]+[MGO-GSH]) mM, and [GSH_{total}] in the assay was (0.1+[MGO-GSH]) mM. One unit of GloI catalyses the formation of 1 μmol of S-D-lactoylglutathione per minute. K_m and V_{max} values were extrapolated from Lineweaver-Burk plots and served for calculating specific activity and k_{cat} values. Kinetic measurements were carried out at 30°C to compare values obtained with those previously reported for human GloI (Ridderström and Mannervik, 1996b).

For measuring GloII activity, the decrease in absorbance resulting from S-D-lactoylglutathione ($\varepsilon_{240\ nm}$=3.1 mM^{-1} cm^{-1}) hydrolysis was measured at 25°C in 100 mM 4-morpholinopropane sulfonate (MOPS) buffer, pH 7.2 in a total volume of 1 ml. S-D-Lactoylglutathione concentrations varied from 0.05 to 0.5 mM; higher concentrations of S-D-lactoylglutathione were limited by its high absorbance at 240. The reaction was started by the addition of GloII. One unit of GloII catalyses the hydrolysis of 1 μmol of S-D-lactoylglutathione per minute. K_m and k_{cat} values of human GloII for S-D-lactoylglutathione were previously reported (Ridderström et al., 1996) using the GloII DTNB [5,5′-dithiobis(2-nitrobenzoate)] assay. The release of 5-thio-2-nitrobenzoate from the reduction of DTNB by GSH (product of the GloII reaction) is monitored spectrophotometrically at 412 nm ($\varepsilon_{412\ nm}$=13.6 mM^{-1} cm^{-1}). Both cGloII and human GloII were tested in the DTNB assay with S-D-lactoylglutathione concentrations ranging from 20 to 1800 μM at 37°C.

Inhibition studies

GloI inhibition was studied at 25°C in the assay system described above. GloII inhibition by S-(*N*-hydroxy-*N*-phenylcarbamoyl)glutathiones was studied in the standard GloII assay. The inhibitors tested differ in the nature of their aryl group, namely S-(*N*-hydroxy-*N*-phenylcarbamoyl)glutathione (HPC-GSH), S-(*N*-hydroxy-*N*-chlorophenylcarbamoyl)glutathione (HCPC-GSH) and S-(*N*-hydroxy-*N*-bromophenylcarbamoyl)-glutathione (HBPC-GSH) (Murthy et al., 1994). *P. falciparum* Glos were directly compared with their human counterparts. S-*p*-Bromobenzylglutathione, a GloI inhibitor for which the diethyl ester prodrug was previously reported to inhibit the growth of *P. falciparum* in culture, with IC_{50} values approximating 5 μM (Thornalley et al., 1994), was also tested as a cGloI inhibitor. The DTNB assay described above was employed for testing weak glyoxalase II inhibitors [namely, S-(*p*-azidophenacyl)glutathione, S-propylglutathione and S-hexylglutathione] which showed high absorbance at 240 nm.

Metal ion analysis

Zinc, iron and nickel contents of both *P. falciparum* glyoxalases II were determined by atomic absorption spectroscopy (Dr. V. Muntean, Seelig Analytical Laboratories, Karlsruhe, Germany). The protein samples were exhaustively dialyzed against 4 mM potassium phosphate buffer, pH 7.0, which also served as a blank in these experiments.

Cultivation of *P. falciparum*

Intraerythrocytic stages of the chloroquine-resistant *P. falciparum* strains K1 and Dd2 were cultured according to Trager and Jensen (1976) with slight modifications. Sorbitol-synchronized parasites in the ring stage were used for testing the effects of two different prodrug forms of HCPC-GSH, namely the HCPC-GSH diethylester and the S-(*N*-hydroxy-*N*-chlorophenylcarbamoyl)sulfoxide on *P. falciparum* in culture. Synchronized parasites (1.5% parasitemia, 3.3% hematocrit, 500 μl total volume) were exposed for 24 h to 0.1–100 μM prodrug. The parasites were then incubated in inhibitor-free medium for another 24 h to complete the *P. falciparum* life cycle of 48 h. Growth inhibition was quantified by counting parasitized red blood cells using Giemsa-stained slides of thin blood smears.

In order to test the effects of Glo inhibitors on Glo activity in the parasites, *P. falciparum* cultures with 15% parasitemia and 3.3% hematocrit were treated for 8 h with 10 μM (2×IC_{50}) S-*p*-bromobenzylglutathione cyclopentyl diester. The parasites were then isolated by suspending the erythrocytes in a 20-fold volume of buffer containing 7 mM K_2HPO_4, 1 mM NaH_2PO_4, 11 mM $NaHCO_3$, 58 mM KCl, 56 mM NaCl, 1 mM $MgCl_2$, 14 mM glucose, and 0.02% saponin (pH 7.5 at 25°C) for 10 min at 37°C. Following centrifugation (1500 *g*, 3 min, 25°C) the pellets were washed three times at 25°C with a 20-fold volume of buffer. The parasites were disrupted by freezing them four times in liquid nitrogen and

thawing, followed by sonication for 2×10 s. After a cleaning spin (135 800 *g*, 60 min, 4°C), the protein content of the parasite extracts was determined using the Bio-Rad (München, Germany) protein dye assay with bovine serum albumin serving as a standard (Bradford, 1976). GloI and GloII activities were determined in the same extracts.

P. falciparum GloI and GloII structure prediction

Models of cGloI, tGloII, and cGloII are based on the crystal structures of homodimeric human glyoxalase I in complex with HIPC-GSH (Cameron et al., 1999a) and human glyoxalase II (Cameron et al., 1999b), respectively (Protein Data Bank accession numbers 1qin and 1qh5, respectively). Alignments were optimized manually in the Swiss-PDB Viewer (spdbv). Computations of the models were carried out at the Swiss-Model server (Guex and Peitsch, 1997; Schwede et al., 2003), and force field energies of the models were calculated with the GROMOS96 implementation of spdbv.

Acknowledgments

The authors wish to thank Elisabeth Fischer and Marina Fischer for their excellent technical support. The study was supported by the Deutsche Forschungsgemeinschaft (Be 1540/4-3 and Schi 102/8-1), the Swedish Research Council and the National Cancer Institute (CA 59612). Monique Akoachere is funded by a scholarship from the Deutscher Akademischer Austauschdienst (DAAD).

References

Antognelli, C., Romani, R., Baldrachini, F., De Santis, A., Andreani, G., and Talesa, V. (2003). Different activity of glyoxalase system enzymes in specimens of S*parus auratus* exposed to sublethal copper concentrations. Chem. Biol. Interact. *142*, 297–305.

Armstrong, R.N. (2000). Mechanistic diversity in a metalloenzyme superfamily. Biochemistry *39*, 13625–13632.

Aronsson, A.C., Sellin, S., Tibbelin, G., and Mannervik, B. (1981). Probing the active site of glyoxalase I from human erythrocytes by use of the strong reversible inhibitor S-*p*-bromobenzylglutathione and metal substitutions. Biochem. J. *197*, 67–75.

Biswas, S., Gairola, C.G., and Das, S.K. (2002). Passive cigarette smoke and the renal glyoxalase system. Mol. Cell. Biochem. *229*, 153–156.

Bradford, M.M. (1976). A rapid and sensitive method for the quantitation of microgram quantities of protein utilizing the principle of protein-dye binding. Anal. Biochem. *72*, 248–254.

Cameron, A.D., Ridderström, M., Olin, B., Kavarana, M.J., Creighton, D.J., and Mannervik, B. (1999a). Reaction mechanism of glyoxalase I explored by an X-ray crystallographic analysis of the human enzyme in complex with a transition state analogue. Biochemistry *38*, 13480–13490.

Cameron, A.D., Ridderström, M., Olin, B., and Mannervik, B. (1999b). Crystal structure of human glyoxalase II and its complex with a glutathione thiolester substrate analogue. Struct. Fold. Des. *7*, 1067–1078.

Clugston, S.L. and Honek, J.F. (2000). Identification of sequences encoding the detoxification metalloisomerase glyoxalase I in microbial genomes from several pathogenic organisms. J. Mol. Evol. *50*, 491–495.

Clugston, S.L., Daub, E., and Honek, J.F. (1998). Identification of glyoxalase I sequences in *Brassica oleracea* and S*porobolus stapfianus*: evidence for gene duplication events. J. Mol. Evol. *47*, 230–234.

Cordell, P.A., Futers, S., Grant, P.J., and Pease, R.J. (2004). The human hydroxyacylglutathione hydrolase (*HAGH*) gene encodes both cytosolic and mitochondrial forms of glyoxalase II. J. Biol. Chem. *279*, 28653–28661.

Creighton, D.J., Zheng, Z.B., Holewinski, R., Hamilton, D.S., and Eiseman, J.L. (2003). Glyoxalase I inhibitors in cancer chemotherapy. Biochem. Soc. Trans. *31*,1378–1382.

Crowder, M.W., Maiti, M.K., Banovic, L., and Makaroff, C.A. (1997). Glyoxalase II from *Arabidopsis thaliana* requires Zn(II) for catalytic activity. FEBS Lett. *418*, 351–354.

Daiyasu, H., Osaka, K., Ishino, Y., and Toh, H. (2001). Expansion of the zinc metallo-hydrolase family of the β-lactamase fold. FEBS Lett. *503*, 1–6.

Frickel, E-M., Jemth, P., Widersten, M., and Mannervik, B. (2001). Yeast glyoxalase I is a monomeric enzyme with two active sites. J. Biol. Chem. *276*, 1845–1849.

Gardner, M.J., Hall, N., Fung, E., White, O., Berriman, M., Hyman, R.W., Carlton, J.M., Pain, A., Nelson, K.E., Bowman, S., et al. (2002). The genome sequence of the human malaria parasite *Plasmodium falciparum*. Nature *419*, 498–511.

Greenwood, B. and Mutabwinga, T. (2002). Malaria in 2002. Nature *415*, 670–672.

Guex, N. and Peitsch, M.C. (1997). SWISS-MODEL and the Swiss-PdbViewer: an environment for comparative protein modeling. Electrophoresis *18*, 2714–2723.

Hamilton, D.S. and Creighton, D.J. (1992). Inhibition of glyoxalase I by the enediol mimic S-(*N*-hydroxy-*N*-methylcarbamoyl)glutathione – the possible basis of a tumor-selective anticancer strategy. J. Biol. Chem. *267*, 24933–24936.

Hamilton, D.S., Kavarana, M.J., Sharkey, E.M., Eiseman, J.L., and Creighton, D.J. (1999). A new method for rapidly generating inhibitors of glyoxalase I inside tumor cells using S-(*N*-aryl-*N*-hydroxycarbamoyl)ethylsulfoxides. J. Med. Chem. *42*, 1823–1827.

Iozef, R., Rahlfs, S., Chang, T., Schirmer, H., and Becker, K. (2003). Glyoxalase I of the malarial parasite *Plasmodium falciparum*: evidence for subunit fusion. FEBS Lett. *554*, 284–288.

Irsch, T. and Krauth-Siegel, R.L. (2004). Glyoxalase II of African trypanosomes is trypanothione-dependent. J. Biol. Chem. *279*, 22209–22217.

Jacobasch, G., Buckwitz, D., Gerth, C., and Thamm, R. (1990). Regulation of the energy metabolism of *Plasmodium berghei*. Biomed. Biochim. Acta *49*, 289–294.

Kalsi, A., Kavarana, M.J., Lu, T., Whalen, D.L., Hamilton, D.S., and Creighton, D.J. (2000). Role of hydrophobic interactions in binding S-(*N*-aryl/alkyl-*N*-hydroxycarbamoyl)glutathiones to the active site of the antitumour target enzyme glyoxalase I. J. Med. Chem. *43*, 3981–3986.

Kavarana, M.J., Kovaleva, E.G., Creighton, D.J., Wollman, M.B., and Eiseman, J.L. (1999). Mechanism-based competitive inhibitors of glyoxalase I: intracellular delivery, *in vitro* antitumor activities, and stabilities in human serum and mouse serum. J. Med. Chem. *42*, 221–228.

Lo, T.W.C. and Thornalley, P.J. (1992). Inhibition of proliferation of human leukaemia 60 cells by diethyl esters of glyoxalase inhibitors *in vitro*. Biochem. Pharmacol. *44*, 2357–2363.

Lo, T.W.C., Westwood, M.E., McLellan, A.C., Selwood, T., and Thornalley, P.J. (1994). Binding and modification of proteins by methylglyoxal under physiological conditions. A kinetic and mechanistic study with N_α-acetylarginine, N_α-acetylcysteine, N_α-acetyl-lysine, and bovine serum albumin. J. Biol. Chem. *269*, 32299–32305.

Marmstål, E., Aronsson, A.C., and Mannervik, B. (1979). Comparison of glyoxalase I purified from yeast (S*accharomyces cerevisiae*) with the enzyme from mammalian sources. Biochem. J. *183*, 23–30.

Mearini, E., Romani, R., Mearini, L., Antognelli, C., Zucchi, A., Baroni, T., Porena, M., and Talesa, V.N. (2002). Differing expression of enzymes of the glyoxalase system in superficial and invasive bladder carcinomas. Eur. J. Cancer *38*, 1946–1950.

Murthy, N.S.R.K., Bakeris, T., Kavarana, M.J., Hamilton, D.S., Lan, Y., and Creighton, D.J. (1994). S-(*N*-Aryl-*N*-hydroxycarbamoyl)glutathione derivatives are tight-binding inhibitors of glyoxalase I and slow substrates for glyoxalase II. J. Med. Chem. *37*, 2161–2166.

Olliaro, P. (2001). Mode of action and mechanism of resistance for antimalarial drugs. Pharmacol. Ther. *89*, 207–219.

Ridderström, M. and Mannervik, B. (1996a). The primary structure of monomeric yeast glyoxalase I indicates a gene duplication resulting in two similar segments homologous to the subunit of dimeric human glyoxalase I. Biochem. J. *316*, 1005–1006.

Ridderström, M. and Mannervik, B. (1996b). Optimized heterologous expression of the human zinc enzyme glyoxalase I. Biochem. J. *314*, 463–467.

Ridderström, M., Saccucci, F., Hellman, U., Bergman, T., Principato, G., and Mannervik, B. (1996). Molecular cloning, heterologous expression and characterization of human glyoxalase II. J. Biol. Chem. *271*, 319–323.

Ridderström, M., Jemth, P., Cameron, A.D., and Mannervik, B. (2000). The active-site residue Tyr-175 in human glyoxalase II contributes to binding of glutathione derivatives. Biochim. Biophys. Acta *1481*, 344–348.

Schwede, T., Kopp, J., Guex, N., and Peitsch, M.C. (2003). SWISS-MODEL: an automated protein homology-modeling server. Nucleic Acids Res. *31*, 3381–3385.

Sherman, I.W. (1979). Biochemistry of *Plasmodium* (malarial parasites). Microbiol. Rev. *43*, 453–495.

Sommer, A., Fischer, P., Krause, K., Boettcher, K., Brophy, P.M., Walter, R.D., and Liebau, E. (2001). A stress-responsive glyoxalase I from the parasitic nematode *Onchocerca volvulus*. Biochem. J. *353*, 445–452.

Sukdeo, N., Clugston, S.L., Daub, E., and Honek, J.F. (2004). Distinct classes of glyoxalase I. metal specificity of the *Yersinia pestis*, *Pseudomonas aeruginosa* and *Neisseria meningitidis* enzymes. Biochem. J. *384*, 111–117.

Thornalley, P.J. (1993). The glyoxalase system in health and disease. Mol. Aspects Med. *14*, 287–371.

Thornalley, P.J. (1996). Pharmacology of methylglyoxal: formation, modification of proteins and nucleic acids, and enzymatic detoxification–a role in pathogenesis and antiproliferative chemotherapy. Gen. Pharmacol. *27*, 565–573.

Thornalley, P.J. (1998). Glutathione dependent detoxification of α-oxoaldehydes by the glyoxalase system: involvement in disease mechanisms and antiproliferative activity of glyoxalase I inhibitors. Chem. Biol. Interact. *111–112*, 137–151.

Thornalley, P.J., Strath, M., and Wilson, R.J.M. (1994). Antimalarial activity *in vitro* of the glyoxalase I inhibitor diester, S-*p*-bromobenzylglutathione diethyl ester. Biochem. Pharmacol. *47*, 418–420.

Thornalley, P.J., Edwards, L.G., Kang, Y., Wyatt, C., Davies, N., Ladan, M.J., and Double, J. (1996). Antitumour activity of S-*p*-bromobenzylglutathione cyclopentyl diester *in vitro* and *in vivo*. Biochem. Pharmacol. *51*, 1365–1372.

Trager, W. and Jensen, J.B. (1976). Human malaria parasites in continuous culture. Science *193*, 673–675.

Vaca, C.E., Fang, J.L., Conradi, M., and Hou, S.M. (1994). Development of a 32P-postlabelling method for the analysis of 2′-deoxyguanosine-3′-monophosphate and DNA adducts of methylglyoxal. Carcinogenesis *15*, 1887–1894.

Vander Jagt, D.L., Han, L-P.B., and Lehman, C.H. (1972). Kinetic evaluation of substrate specificity in the glyoxalase-I-catalyzed disproportionation of α-ketoaldehydes. Biochemistry *11*, 3735–3740.

Wenzel, N.F., Carenbauer, A.L., Pfiester, M.P., Schilling, O., Meyer-Klaucke, W., Makaroff, C.A., and Crowder, M.W. (2004). The binding of iron and zinc to glyoxalase II occurs exclusively as di-metal centers and is unique within the metallo-β-lactamase family. J. Biol. Inorg. Chem. *9*, 429–438.

Zuegge, J., Ralph, S., Schmuker, M., McFadden, G.I., and Schneider, G. (2001). Deciphering apicoplast targeting signals – feature extraction from nuclear-encoded precursors of *Plasmodium falciparum* apicoplast proteins. Gene *280*, 19–26.

Received October 11, 2004; accepted November 19, 2004